iFEM2.0: Dense 3D Contact Force Field Reconstruction and Assessment for Vision-based Tactile Sensors (Extended Abstract)

Can Zhao[1], JinLiu[2], and Daolin Ma[1]

***Abstract*— Vision-based tactile sensors offer rich tactile information through high-resolution tactile images, enabling the reconstruction of dense contact force fields on the sensor surface. However, accurately reconstructing the three-dimensional (3D) contact force distribution remains a challenge. In this paper, we propose the multi-layer inverse finite element method (iFEM2.0) as a robust and generalized approach to reconstruct dense contact force distribution. We systematically analyze various parameters within the iFEM2.0 framework, and determine the appropriate parameter combinations through simulation and in-situ mechanical calibration. Our approach incorporates multi-layer mesh constraints and ridge regularization to enhance robustness. Furthermore, as no off-the-shelf measurement equipment or criterion metrics exist for 3D contact force distribution perception, we present a benchmark covering accuracy, fidelity, and noise resistance that can serve as a cornerstone for other future force distribution reconstruction methods. The proposed iFEM2.0 demonstrates good performance in both simulation- and experiment-based evaluations. Such dense 3D contact force information is critical for enabling dexterous robotic manipulation that handles both rigid and soft materials.**

I. INTRODUCTION

Robots are increasingly performing complex tasks such as surgical assistance, space servicing, and precision assembly [1]–[3]. In these unstructured environments, dense 3D contact force perception is critical for ensuring safe and effective interaction [4], [5], offering valuable insights into object properties like texture, stiffness, and friction [6]–[9]. While traditional tactile sensors excel at normal force sensing [10]–[12], tangential force measurement is essential for capturing frictional behaviors and detecting slippage [13], [14], particularly when manipulating deformable objects [15], [16]. Fig. 1 illustrates a practical scenario showcasing the importance of dense 3D contact force fields. In this example, the softer outer contact region induces smaller tangential forces on the sensor, whereas the stiffer central part exhibits larger tangential forces, which aligns with Hertzian contact [17] and friction principles [18]. Such nuanced information allows for better perceiving and manipulating rigid-soft coupled objects.

Vision-based tactile sensors [19], [20] offer promising hardware, capable of recovering the surface deformation fields, while accurately estimating the contact force distribution from the deformation fields poses a challenge. This inverse mechanical problem is inherently ill-conditioned, leading to serious errors even with minor measurement noise [21]. Existing methods for reconstructing contact force via vision-based tactile sensors often yield noisy results [22]–[24]. Furthermore, the lack of standardized benchmarks hampers method evaluation and comparison.

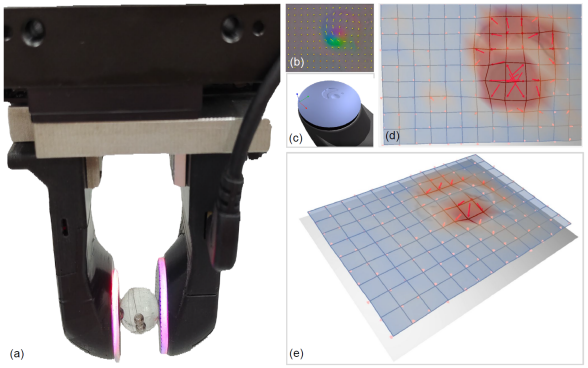

Fig. 1. An example of dense 3D contact force fields for perceiving rigid-soft coupled objects through tangential force distributions between central and outer region. (a) The GelSlim 3.0 sensor holds onto a coupled rigid-soft ball. (b) 2D tangential displacement field. (c) Depth field. (d) 3D contact force field with noise reconstructed using raw iFEM. (e) Enhanced accuracy and clarity in the 3D contact force field reconstructed via iFEM 2.0.

In this study, we propose iFEM2.0, a comprehensive and robust method for reconstructing dense contact force fields using vision-based tactile sensors.

- **Accurate and Robust Algorithm** to reconstruct dense, precise and robust 3D contact force distribution are proposed. The framework leverages a multi-layer mesh with complementary constraints and regularization mechanisms to effectively address model inaccuracies and ill-conditioning issues while handleing measurement noise.
- **Appropriate Model Parameter Combination** about the constitutive models, element parameters, and material properties of tactile sensors are determined within iFEM2.0 through comprehensive simulation comparisons and in-situ mechanical calibration.
- **Integrated Evaluation Benchmark and Metrics** for 3D contact force reconstruction are established, covering accuracy, fidelity, noise resistance and generalizability. The iFEM2.0 demonstrates superior performance in both simulation- and experiment-based evaluations compared with previous methods.

C. Zhao, D. Ma are with the School of Ocean & Civil Engineering, Shanghai Jiao Tong University, Shanghai 200240, China (e-mail: can.zhxx, daolinma@sjtu.edu.cn). J. Liu is with the School of Mechanical Engineering, Shanghai Jiao Tong University, Shanghai 200240, China (e-mail: jinliu.sjtu@outlook.com). *(Corresponding author: Daolin Ma)*

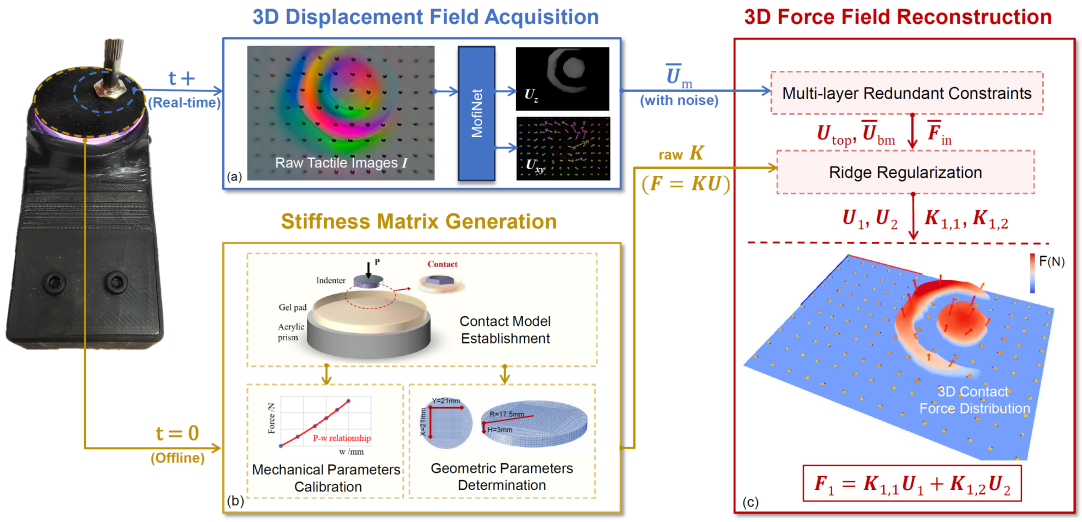

Fig. 2. Algorithm flowchart for 3D contact force distribution. (a) 3D displacement field acquisition from tactile images using a neural network. (b) Stiffness matrix generation: contact model establishment, mechanical parameters calibration, and geometric parameters determination of vision-based tactile sensor. (c) 3D contact force field (normal and tangential) reconstruction from noisy 3D displacement field and original stiffness matrix.

II. Method

In this section, we present details of the iFEM2.0 algorithm, as shown in Fig. 2.

First, key notations are described to clearly define the problem. The gel pad of sensor is discretized into a multi-layer uniform 8-node hexahedral element system, with n_e element layers and n_p node layers ($n_e \geq 2$, $n_p = n_e + 1$). The displacement and force vectors for the entire system are denoted as $\boldsymbol{U} = \{\boldsymbol{U}_1{}^T, \boldsymbol{U}_2{}^T, \ldots, \boldsymbol{U}_{n_p}{}^T\}^T$ and $\boldsymbol{F} = \{\boldsymbol{F}_1{}^T, \boldsymbol{F}_2{}^T, \ldots, \boldsymbol{F}_{n_p}{}^T\}^T$. The observed 3D displacement field on the outer surface of gel pad is denoted as $\overline{\boldsymbol{U}}_m$. The goal is to reconstruct the 3D contact force distribution on the pad's surface $\boldsymbol{F}_1 = \mathcal{G}(\overline{\boldsymbol{U}}_m)$.

Reconstructing the 3D contact force distribution $\boldsymbol{F}_1$ from noisy surface nodal displacements $\overline{\boldsymbol{U}}_m$ is challenging, as directly reversing the forward contact model for vision-based tactile sensors is inherently ill-conditioned and often unfeasible. To address this, we propose the multi-layer inverse finite element method (iFEM2.0) to reconstruct $\boldsymbol{F}_1$ and enhance the effect by incorporating a ridge regularization term.

1) Specific Boundary Conditions: We first define a simplified contact model with the following assumptions:

- The reconstruction is limited to the central gel region to avoid peripheral image distortion.
- The built-in camera records real-time deformation of the gel pad's top surface, i.e., $\boldsymbol{U}_1 = \overline{\boldsymbol{U}}_{top} \approx \overline{\boldsymbol{U}}_m$ (with noise). The bottom surface is adhered to the acrylic prism, treated as a rigid foundation, i.e., $\boldsymbol{U}_{n_p} = \overline{\boldsymbol{U}}_{bm} = 0$.
- External loads applied to intermediate-layer nodes are zero, i.e., $\boldsymbol{F}_2 = \cdots = \boldsymbol{F}_{n_{p-1}} = 0$.

2) Multi-layer Inverse Finite Element Method: The discrete silica gel system consists of n_p layers of nodes ($n_p = n_e + 1$, $n_e \geq 2$). For the only two-layer element case ($n_e = 2$), incorporating boundary conditions into the finite element equilibrium $\boldsymbol{KU} = \boldsymbol{F}$ results in equations:

$$\boldsymbol{K}_{2,2}\boldsymbol{U}_2 = -\boldsymbol{K}_{2,1}\boldsymbol{U}_1, \boldsymbol{F}_1 = \boldsymbol{K}_{1,1}\boldsymbol{U}_1 + \boldsymbol{K}_{1,2}\boldsymbol{U}_2. \quad (1)$$

For systems more than two layers ($n_e \geq 3$), the intermediate-layer displacement distribution are condensed as$\boldsymbol{U}_2'$. The corresponding matrices are denoted as $\boldsymbol{K}_{1,2}'$, $\boldsymbol{K}_{2,1}'$, and $\boldsymbol{K}_{2,2}'$, respectively. For simplicity, we use the same notation for ($\boldsymbol{U}_2'$, $\boldsymbol{K}_{1,2}'$, $\boldsymbol{K}_{2,1}'$ and $\boldsymbol{K}_{2,2}'$), as the original variables ($\boldsymbol{U}_2$, $\boldsymbol{K}_{1,2}$, $\boldsymbol{K}_{2,1}$ and $\boldsymbol{K}_{2,2}$). However, inverting $\boldsymbol{K}_{2,2}$ is ill-conditioned due to its large sparse nature, leading to potential fluctuations in force calculations [21]. Moreover, measurement noise in the upper node displacement observations $\overline{\boldsymbol{U}}_m$ further affects the accuracy of force calculation results.

3) Ridge Regularization: To address the ill-conditioning, Ridge regularization is chosen due to its benefits in enhancing stability, ease of use, and numerical efficiency, particularly for solving inverse problems [21], [25]. Ridge regularization introduces L_2 regularization term to the loss function, transforming the force reconstruction into an optimization problem. The optimization objective is formulated as: $arg\min_{\boldsymbol{U}_2} \|\boldsymbol{K}_{2,1}\boldsymbol{U}_1 + \boldsymbol{K}_{2,2}\boldsymbol{U}_2\|_2^2 + \lambda\|\boldsymbol{U}_2\|_2^2$.

Solving this convex function by setting its derivative to zero, resulting in the estimation of $\boldsymbol{U}_2$ as:

$$\boldsymbol{U}_2 = (\boldsymbol{K}_{2,2}{}^T\boldsymbol{K}_{2,2} + w\boldsymbol{I})^{-1}\boldsymbol{K}_{2,2}{}^T(-\boldsymbol{K}_{2,1}\boldsymbol{U}_1 + \boldsymbol{n}_0) \quad (2)$$

where w and $\boldsymbol{n}_0$ denote a regularization parameter and the noise level, respectively.

III. Conclusion

In this study, we present iFEM2.0, a multi-layer inverse finite element method designed to enhance the accuracy and robustness of contact force reconstruction for vision-based tactile sensors. Our framework enables precise estimation of 3D contact force distributions—including both normal and tangential components—at each measurement point. This method holds broad potential for advanced closed-loop strategies in robot control.

REFERENCES

[1] K. Nozu and K. Shimonomura, "Robotic bolt insertion and tightening based on in-hand object localization and force sensing," in *2018 IEEE/ASME International Conference on Advanced Intelligent Mechatronics (AIM)*, pp. 310–315, 2018.

[2] H. seok Song, K. young Kim, and J. ju Lee, "Development of the dexterous manipulator and the force sensor for minimally invasive surgery," in *2009 4th International Conference on Autonomous Robots and Agents*, pp. 524–528, 2009.

[3] Z. Jiang, X. Cao, X. Huang, H. Li, and M. Ceccarelli, "Progress and development trend of space intelligent robot technology," *Space: Science & Technology*, 2022.

[4] Y. Ding, F. Wilhelm, L. Faulhammer, and U. Thomas, "With proximity servoing towards safe human-robot-interaction," in *2019 IEEE/RSJ International Conference on Intelligent Robots and Systems (IROS)*, pp. 4907–4912, 2019.

[5] A. Zacharaki, I. Kostavelis, A. Gasteratos, and I. Dokas, "Safety bounds in human robot interaction: A survey," *Safety science*, vol. 127, p. 104667, 2020.

[6] N. Jamali and C. Sammut, "Material classification by tactile sensing using surface textures," in *2010 IEEE International Conference on Robotics and Automation*, pp. 2336–2341, 2010.

[7] J. M. Romano and K. J. Kuchenbecker, "Methods for robotic tool-mediated haptic surface recognition," in *2014 IEEE Haptics Symposium (HAPTICS)*, pp. 49–56, IEEE, 2014.

[8] S. Luo, J. Bimbo, R. Dahiya, and H. Liu, "Robotic tactile perception of object properties: A review," *Mechatronics*, vol. 48, pp. 54–67, 2017.

[9] W. Li, A. Alomainy, I. Vitanov, Y. Noh, P. Qi, and K. Althoefer, "F-touch sensor: Concurrent geometry perception and multi-axis force measurement," *IEEE Sensors Journal*, vol. 21, no. 4, pp. 4300–4309, 2020.

[10] Y. Yan, Z. Hu, Z. Yang, W. Yuan, C. Song, J. Pan, and Y. Shen, "Soft magnetic skin for super-resolution tactile sensing with force self-decoupling," *Science Robotics*, vol. 6, no. 51, p. eabc8801, 2021.

[11] M. Yang, Y. Cheng, Y. Yue, Y. Chen, H. Gao, L. Li, B. Cai, W. Liu, Z. Wang, H. Guo, *et al.*, "High-performance flexible pressure sensor with a self-healing function for tactile feedback," *Advanced Science*, vol. 9, no. 20, p. 2200507, 2022.

[12] C. Yang, L. Li, J. Zhao, J. Wang, J. Xie, Y. Cao, M. Xue, and C. Lu, "Highly sensitive wearable pressure sensors based on three-scale nested wrinkling microstructures of polypyrrole films," *ACS applied materials & interfaces*, vol. 10, no. 30, pp. 25811–25818, 2018.

[13] W. Yuan, R. Li, M. A. Srinivasan, and E. H. Adelson, "Measurement of shear and slip with a gelsight tactile sensor," in *2015 IEEE International Conference on Robotics and Automation (ICRA)*, pp. 304–311, 2015.

[14] C. Melchiorri, "Slip detection and control using tactile and force sensors," *IEEE/ASME transactions on mechatronics*, vol. 5, no. 3, pp. 235–243, 2000.

[15] H. Yin, A. Varava, and D. Kragic, "Modeling, learning, perception, and control methods for deformable object manipulation," *Science Robotics*, vol. 6, no. 54, p. eabd8803, 2021.

[16] Y. Wi, P. Florence, A. Zeng, and N. Fazeli, "Virdo: Visio-tactile implicit representations of deformable objects," in *2022 International Conference on Robotics and Automation (ICRA)*, pp. 3583–3590, 2022.

[17] H. Hertz, "The contact of elastic solids," *J Reine Angew, Math*, vol. 92, pp. 156–171, 1881.

[18] B. N. Persson, *Sliding friction: physical principles and applications*. Springer Science & Business Media, 2013.

[19] W. Yuan, S. Dong, and E. H. Adelson, "Gelsight: High-resolution robot tactile sensors for estimating geometry and force," *Sensors*, vol. 17, no. 12, p. 2762, 2017.

[20] E. Donlon, S. Dong, M. Liu, J. Li, E. Adelson, and A. Rodriguez, "Gelslim: A high-resolution, compact, robust, and calibrated tactile-sensing finger," in *2018 IEEE/RSJ International Conference on Intelligent Robots and Systems (IROS)*, pp. 1927–1934, 2018.

[21] C. M. Le, K. Levin, P. J. Bickel, and E. Levina, "Comment: Ridge regression and regularization of large matrices," *Technometrics*, vol. 62, no. 4, pp. 443–446, 2020.

[22] Y. Zhang, Z. Kan, Y. Yang, Y. A. Tse, and M. Y. Wang, "Effective estimation of contact force and torque for vision-based tactile sensors with helmholtz–hodge decomposition," *IEEE Robotics and Automation Letters*, vol. 4, no. 4, pp. 4094–4101, 2019.

[23] C. Sferrazza and R. D'Andrea, "Design, motivation and evaluation of a full-resolution optical tactile sensor," *Sensors*, vol. 19, no. 4, p. 928, 2019.

[24] D. Ma, E. Donlon, S. Dong, and A. Rodriguez, "Dense tactile force estimation using gelslim and inverse fem," in *2019 International Conference on Robotics and Automation (ICRA)*, pp. 5418–5424, 2019.

[25] A. N. Tikhonov, "Solution of incorrectly formulated problems and the regularization method.," *Sov Dok*, vol. 4, pp. 1035–1038, 1963.